# ATLAS NOTE

ATL-PHYS-PUB-2009-XXX

March 27, 2009

## Measurement of Lorentz angle and depleted depth in the ATLAS Pixel Detector with cosmics data

The ATLAS Collaboration

### Abstract

Cosmic ray data taken during the ATLAS combined cosmics runs of the Fall 2008 have been used to measure the value of the Lorentz angle and of the depleted depth for the Pixel Detector.

The value of the Lorentz angle in the pixel detector depends on the operating conditions (bias voltage and temperature) and on the magnetic field. It can be measured from the track incidence angle which corresponds to the minimum width of pixel clusters. We find that for the Pixel detector barrel the average value of the Lorentz angle in the local R$\phi$ direction is $(214.7 \pm 0.4 \pm Z.Z)$ mrad, consistent with expectations. The expected dependence of the Lorentz angle on the operating temperature and on the value of the local magnetic field have also been observed.

The increase of cluster size with incidence angle is sensitive to the value of the depleted depth. Two independent methods have been used to measure the depleted depth using cosmics data without magnetic field. They both find values in agreement with the expected sensor thickness of 253 $\mu$m.

# 1 Introduction

Both resolution and hit efficiency of the Pixel Detector are affected by variations in the amount of collected charge and charge-sharing among the neighbouring pixels. Optimal resolution is achieved when charges deposited by the traversing particle is spread over two pixels and an interpolation algorithm is used in determining the point where the particle crossed the sensor. Charge sharing is determined by the depth of the depleted region, the Lorentz angle, and the angle of the sensor with respect to the incident particles.

Because of the Lorentz force, the charge carriers in the pixel sensors do not drift directly toward the electrodes, but in a direction which forms an angle, called Lorentz angle, with respect to the normal. In the disks the magnetic field component perpendicular to the electric field is very small, hence this effect is relevant only for the barrel, where the Lorentz force is along the local $R\phi$ direction. The Lorentz angle is a function of the magnetic field and the electron mobility in silicon, which depends on the bias voltage, the active thickness, and the temperature [1–3].

The effect of the Lorentz force is a shift in the position where charge is collected at the surface with respect to where it has been released by the particle. This needs to be properly taken into account in the reconstruction of the pixel data, or it would be interpreted as a shift by the alignment algorithms. The Lorentz angle also influences the angular dependence of the cluster size on the track incidence angle, and this property is used in the measurements reported in this paper. Similar measurements have also been made with testbeam data [2, 3].

The depleted region is expected currently to be equal to the sensor thickness, since the bias voltage required for full depletion of the production sensor is of the order of 40 V *check the true value, any reference?* while the operating bias voltage is 150 V. Radiation damage will eventually increase the effective doping concentration of silicon [1)] and thus full depletion voltage [**?**]. Eventually when the full depletion voltage exceedd the maximum operating bias voltage of about 600 V, the sensors will only be partially depleted. *check the exact fluence/luminosity at which this is expected.* One of the purposes of the measurements described here is the development of techniques to monitor the evolution of the depletion depth of the sensors.

The depleted thickness influences the amount of charge collected. For particles crossing the sensor at an angle $\phi$ with respect to the normal, it also influences the charge sharing between pixel cells and the width of the resulting pixel clusters.

This note describes two techniques used to measure the depletion depth with the cosmic ray data. The first is based on a comparison of the observed dependence of the cluster width on the angle of incidence with the predictions of the full detector simulation for different depletion depths. The second technique uses the reconstructed particle trajectory to compute the depth of the charge released in each sensor. A similar method was used in the past to measure the depletion depth with the testbeam data [2, 3].

In Section 2 the real and simulated data samples used in the analysis are described. The common selections of good tracks are also presented. In Section 3 the measurement of Lorentz angle is described. Section 4.1 presents the measurements of depletion depth from the cluster size, while Section 4.2 explains the measurement using the depth of the charge deposits. Conclusions are reported in Section 5.

# 2 Data samples and selections

## 2.1 Data samples

Three groups of data have been used:

[1)] Initially the effective doping concentration will actually decrease. It will increase after the radiation-induced type-nversion of the initial n-type pixel sensors.

Table 1: List of runs used in the analysis.

| Data Set | runs |
|---|---|
| ATLAS combined data (B-on) | 90262, 90264, 90270, 90731, 90732, 90733, 90749, 90757, 90758, 90784, 90786, 90792, 91361, 91389, 91391, 91400, 91464, 91636, 91639, 91800, 91801, 91808, 91860, 91861, 91885, 91888, 91890, 91891, 91900, 92082 |
| ATLAS combined data (B-off) | 89740, 89851, 90943, 91059, 91060, 92045, 92048, 92051, 92057 |
| ID combined data (B-off) | 96542, 96544, 96582, 96696, 96858, 96884, 96895, 96903 |

Table 2: Statistics of the data used in the analysis. The second column reports the number of tracks, the second column the number of clusters on track, and the third column the number of clusters on track which pass the common selection cuts.

| Data Set | $N_{Tr}$ | $N_{Cl}$ | $N_{Cl}^{\text{good}}$ |
|---|---|---|---|
| ATLAS combined data (B-on) | 134524 | 510292 | 332023 |
| ATLAS combined data (B-off) | | | |
| ID combined data (B-off) | | | |
| simulation (B-on) | | | |
| simulation (B-off) | | | |

- Data from the ATLAS combined runs of September/October 2008, with the solenoidal magnetic field on. The IDCosmic trigger stream was used. The list of runs is reported in the first row of Table 1.
- Data from the ATLAS combined runs of September/October 2008, with the solenoidal magnetic field off. This is a control sample, to verify wether a Lorentz angle consistent with zero is found. The IDCosmic trigger stream was used. The list of runs is reported in the second row of Table 1.
- Data from the ID combined runs of November 2008, with the solenoidal magnetic field off. The TRT trigger stream was used. The list of runs is reported in the third row of Table 1.

For all of them, the DPD_PIXELCOMM datasets produced in the first reprocessing were used (tag o4_r602_p16). These datasets contain events filtered with the requirement of at least one pixel hit. The number of tracks and pixel cluster on track on the data are reported in Table 2. All events have been reconstructed with the offline release 15.0.0. The New Tracking algorithm is used to reconstruct tracks.

Cosmic Montecarlo datasets have also been used. The simulated cosmic raw hit are simulated using Atlas-GEO-03-00-00. These hits are digitized using release 15.0.0 and with Atlas Geomentry-07-00-00 and also reconstructed in the same release. The same reconstruction procedure is used for cosmic data and simulated MC. A total of 50 000 events with solenoid field on and 50 000 events with solenoid field off have been used. The resulting statistics of simulated tracks is shown in Table 2.

### 2.2 Track selection

Pixel clusters associated to a track were selected, which satisfy the following conditions:

- The residual between the track and the cluster is less than 1 mm in absolute value, for each local coordinate.
- In adition to the cluster associated to the track, no other cluster is present in the Pixel Detector module.
- No ganged pixel is included in the cluster
- The first two rows and colums of pixels at the edge of a module are rejeceted.
- The extrapolated position of the cluster $x_c$ must be located between the first and the last hit pixel.
- The track polar incidence angle is less than 45 degrees.

The number of pixel hits on tracks which passes the above requirements is also reported in Table 2.

## 3 Measurement of Lorentz angle

In the presence of an electric field, $E$, and a magnetic field, $B$, the charge carriers liberated by a passing particle within silicon drift along a direction at an angle $\alpha_L$ (Lorentz angle) with respect to the electric field direction (due to the $\vec{E} \times \vec{B}$ effect). They usually spread over several pixels, dependending on the angle of the incident particle. This spread is a minimum for an angle equal to the Lorentz angle as shown schematically in Fig. 1. This property is the base of the measurement reported here.

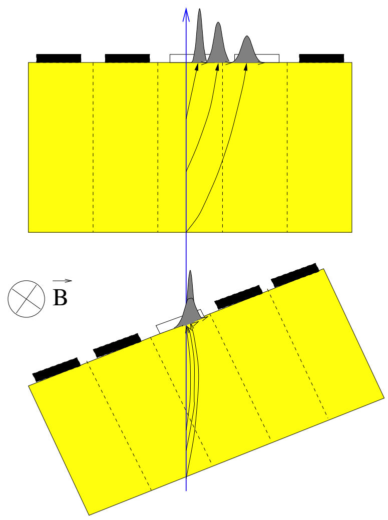


Figure 1: Drift of charge carriers under the influence of a magnetic field. The upper figure shows a perpendicular particle, in the lower figure the incident particle crosses the sensor at an angle equal to the Lorentz angle.

The value of the Lorentz angle is given by

$$\tan \alpha_L = \mu_H B = r\mu B \qquad (1)$$

where

$\mu_H$ is the Hall mobility of the charge carrier in silicon, $\mu$ is the drift mobility and their ratio $r$ (Hall factor) is a pure number close to 1. This depends on the scattering cross section of the charge carriers. More specifically $r = <\tau^2> / <\tau>^2$ where $\tau$ is the mean free time between collisions.

The Hall factor in silicon has a weak dependence on temperature and does not depend on doping levels in the relevant range for the ATLAS silicon detectors. For electrons $r = 1.15$ at 300 °K and $r = 1.12$ at 264 °K. The mobility depends on temperature and electric field while the dependence on impurity concentration is negligible for the values relevant for the ATLAS silicon tracker. Parametrizations of this dependence for electrons and holes in silicon can be found in reference [1]. Those used to correct for the Lorentz shift in the ATLAS reconstruction are reported in [2] and [4].

In the Pixel detector, the relevant Lorentz angle is that of electrons, which are the charge carrier collected on the electrodes. The orientation of the Pixel Detector modules and the magnetic field is such that the Lorentz effect is expected to be significant only for the local $R\phi$ direction in the barrel. During the combined data taking periods of the Fall 2008, the Pixel Detector was operated at a bias voltage of 150 V and at a mean temperature of 269 °K. The average thickness of the sensors, according to the measurements performed during production, is 253 $\mu$m, resulting in an average electric field of 593 kV/m. The solenoidal magnetic field in the barrel has an average value of 1.994 T. There is a small variation along the beam axis direction, from a minimum of 1.984 T to a maximum of 1.998 T, while the radial dependence is negligible.

The expected Lorentz angle value in these conditions is 225 mrad. The dominant uncertainty on this value comes from the uncertainty on the value of electron mobility in silicon, and it is about 5%.

### 3.1 Results

In order to measure the Lorentz angle in the local $R\phi$ direction for the Pixel Detector barrel, the cluster width in this direction (i.e. the number of rows) has been studied as a function of the incidence angle in the plane defined by the local $R\phi$ direction and the normal to the sensor surface.

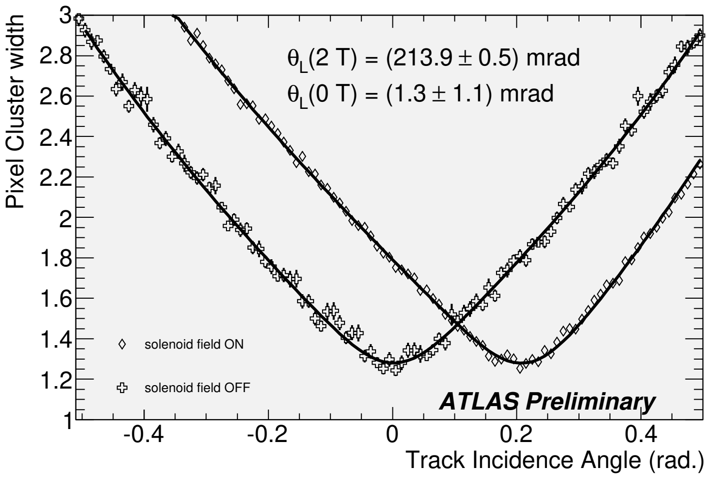


Figure 2: Width of the pixel clusters as a function of the track incidence angle in the $R\phi$ plane. The two curves refere to cosmics data taken with and without the solenoidal magnetic field. The fitting function (described in the text) is superimposed.

In Fig. 2 the cluster width is reported as a function of the incidence angle. Data taken with and

Table 3: Summary of Lorentz Angle fit to the cosmic data and MC. The first uncertainty is statistical, the second systematic.

| Data Set | Slope | Smearing | Lorentz Angle (mrad) | Minimum Cluster Size |
|---|---|---|---|---|
| Data (b-on) | 3.192 ± 0.010 | 0.065± 0.004 | 214.7 ± 0.4 | 1.089 ± 0.005 |
| Data (b-off) | 3.195 ± 0.012 | 0.074± 0.004 | -0.3 ± 0.8 | 1.088 ± 0.006 |
| MC (b-on) | 3.14 ± 0.03 | 0.065± 0.011 | 236.0 ± 2.0 | 1.04 ± 0.02 |
| MC (b-off) | | $10^{+4.1}_{-3.4}$ | 1.0 | |
| MC (th-3705 b-on) | 3.170 ± 0.034 | 0.051± 0.015 | 285 ± 2 | 1.052 ± 0.016 |

without magnetic field are considered separately. The effect of the Lorentz force to shift the angular position corresponding to the minimum cluster width is evident. The curve has been fitted with the following function:

$$(a*(\tan(\alpha)-\tan(\alpha_L))+b/\cos(\alpha))\oplus G(\alpha) \tag{2}$$

where $\oplus$ indicates the convolution operator, $G$ the gaussian function, while $a$ and $b$ are parameters of the fit. $\alpha_L$ yields the Lorentz angle value. The parameter $a$ is a measure of how rapidly the cluster size increases with the incidence angle and it can be used to measure the depleted depth, as described in Section 4.1.

The fit provides a Lorentz angle value of $(214.7\pm0.4)$ mrad for the data with magnetic field, and $(1.3\pm1.1)$ mrad for the data without magnetic field. They are consistent with the expected values of $(225\pm11)$ mrad and 0 respectively.

In Fig. 3 the cluster size dependence on the track angle is reported for data and simulation with magnetic field. It can be seen that the agreement is fairly good in the range of incidence angle relevant for the Lorentz angle measurement.

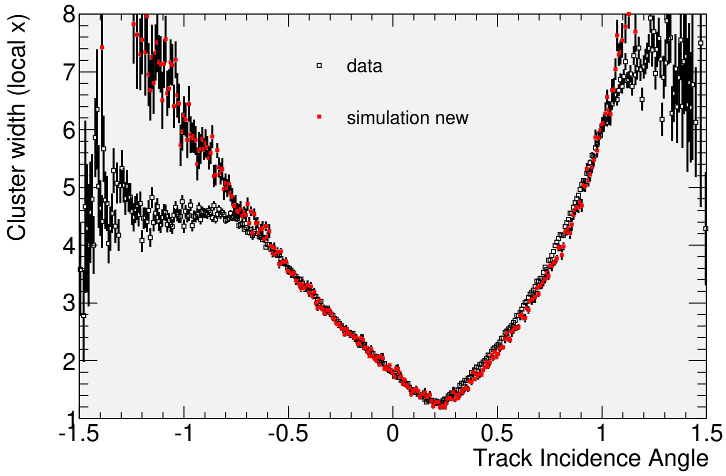


Figure 3: Width of the pixel clusters as a function of the track incidence angle in the $R\phi$ plane. The open points are cosmics ray data. The closed point are the cosmics MC result.

The fit of the simulated data provides a Lorentz angle of $(XXX \pm YYY)$ mrad. This should be compared with the true value used in the simulation, which was ZZZ mrad. *Some comments ?*

*Lorentz angle z and disks - maybe*

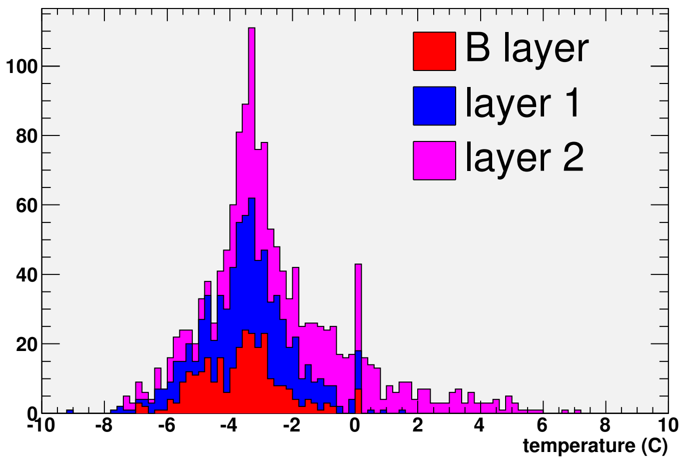


Figure 4: Temperature of the pixel modules in the barrel.

The Lorentz angle dependence on the temperature can be verified using the data. The temperature of each pixel module is monitored, and this information is available from the conditions database. In Fig. **??** the distribution of the pixel module temperature is shown.

Temperature variations occur between different staves. The highest values are associated for those layer-2 staves with inserted cooling pipes, for which cooling is less efficient. The temperature has been found to be pretty stable between different runs, and shows little variation along the barrel stave. This last property ensures there is little correlation between the temperature and the magnetic field, which has a significant variation along the beam axis.

*Insert field figure here*

In Fig. **??** the magnetic field dependence on the position of modules along the barrel stave and the correlation between magnetic field and temperature are shown. The former is too small to be measured with the available statistics. The latter can be used to correct the measured Lorentz angle dependence on temperature, but it is also a very small effect.

In Fig. 5 the dependence of the measured Lorentz angle on the temperature is shown. There is a clear correlation, and a linear fit gives $d\alpha_L/dT = (-0.78 \pm 0.18) mrad/^{\circ}C$. When the magnetic field effect is corrected for, a value of $d\alpha_L/dT = (ZZ \pm ZZ)$ mrad/°C is found. This is consistent with the expected value of 0.ZZ mrad/°C

### 3.1.1 Systematic uncertainties

Some description of systematics uncertainties. Preliminary list:

- Consistency with 0 of the result of the fit when no Lorentz effect is expected ($\vec{B}$ parallel to $\vec{E}$ or no $\vec{B}$)
- Consistency of true and simulated Lorentz angle in the simulation. This also tests any effect on Lorentz angle from the charge collection and electronics effect included in the simulation, such as threshold, cross talk, and diffusion.

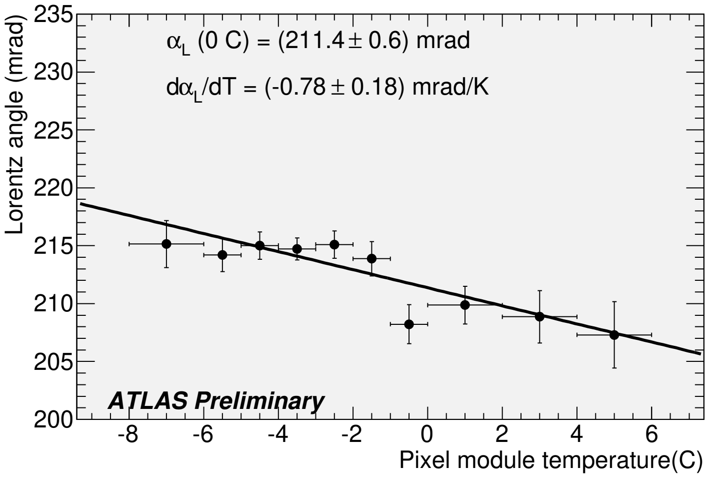


Figure 5: Measured Lorentz angle as a function of the pixel module temperature.

- Variation of Lorentz angle with fit range

### 3.2 Discussion

*Some discussion?*

# 4 Measurement of depleted depth

### 4.1 Measurement using cluster size

The value of the depletion of Pixel detector was extracted from the slope parameter of the Lorentz fits. The relation between the slope parameter and the value of depletion depth was determined from the simulation of data with different depleted depth. This takes into accout the effect of threshold, diffusion, and cross talk on the cluster size.

The values of the slope parameter found in the simulation and in the data are reported in Table 3. The values found in field on and in field off data are in agreement. The simulated value is in agreement with the data, which indicates that the depletion value is close to the simulated one (250 $\mu$m as expected). In order to measure the depleted depth, we have measured the slope parameter with a MC sample with a depleted depth of 200 $mu$m. (*report the results in table 3 or maybe in a separate table here. A plot with slope vs depletion in Montecarlo, the systematics band due to the threshold variation, and the horizonatal band from the measurement on data may also be a pretty way to display results.*

The variation of the slope parameter $S$ on the depletion depth $D$ is thus $dS/dD = (\pm)\mu\text{m}^{-1}$. We can thus derive the depletion depth by comparing the slope parameter in the data $(S_{data})$ with the one in the Montecarlo $(S_{MC})$:

$$D = D_{MC} + dD/dS \cdot (S_{data} - S_{MC}) \tag{3}$$

This gives D = , where the error is only statistical.

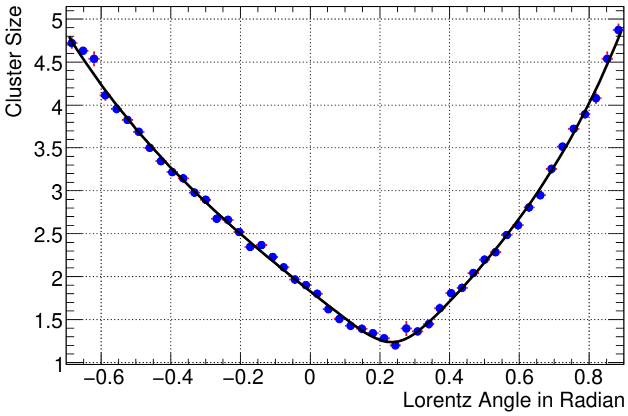


Figure 6: The Lorentz angle distribution from MC simulated data with threshold 3705 electron. points with error bars represents the data and solid line the fitted function. The error bars represents only statistical error only.

#### 4.1.1 systematic uncertainties

.

*We have checked*

*- Change of slope parameter when changing the threshold within the uncertainty from charge scale, assumed to be 5%.*

*- we may have to play with diffusion and cross talk to show the uncertainty related to those is indeed very small*

*So far the effect on slope is negligible within the statistics of MC data. This is good!*

### 4.2 Measurement using charge depth

#### 4.2.1 Measurement Method

Particle tracks can be used to measure the depletion depth. Therefore it is necessary to know the cluster size, the incident angle and the entry point of the particle. The entry point is the point where the particle hits the surface of the sensor on the pixel side. The size of a pixel cluster depends on the amount of pixels which collect enough charge to reach the threshold. The size of the sensitive region depends on the depletion depths. Therefore the cluster size depends on the depth of the depleted zone.

To simplify matters only clusters in short pixel direction are regarded. A scheme of the pixel sensor in the R$\phi$ plane is shown in Figure 7. $L$ is the thickness of the pixel sensor and $D$ is the true depletion depth of the pixel sensor. The track incidence angle $\alpha$ is measured relative to the normal of the pixel plane. The tracking algorithm determines the residual $s$ between the centre of the cluster and the particle track. This information is used to calculate the extrapolated cluster position $x_c$. Therewith it is possible to estimate the entry point $x_0$ of the track. The extrapolated cluster position $x_c$ is calculated for the centre of the depleted depth. Hence the local z-coordinate for this value is $\frac{D}{2}$.

The entry point is calculated with the following formula:

$$x_0 = x_c - \frac{D}{2} \tan \alpha \ . \tag{4}$$

Since the depletion depth is unknown, $D$ is replaced by the depth $L$ of the sensor:

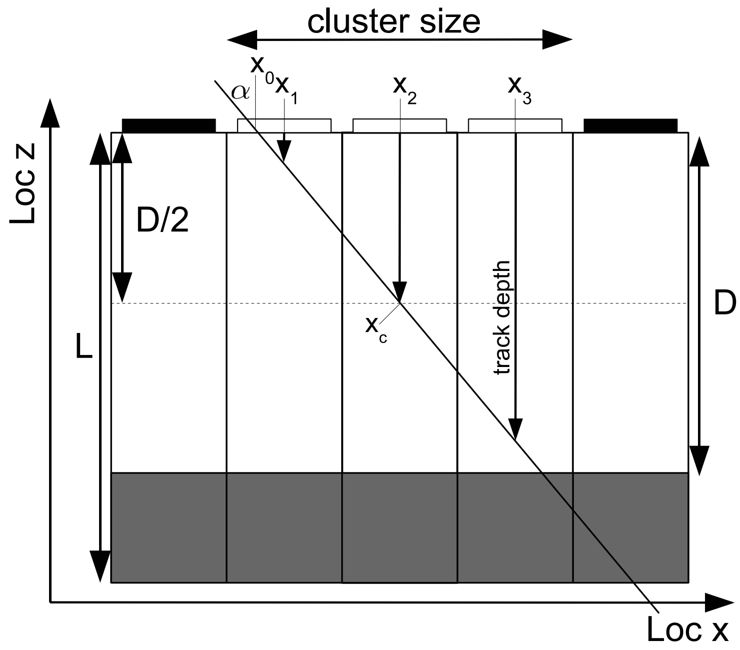


Figure 7: Schematic view of a particle crossing the pixel sensor

$$x_0' = x_c - \frac{L}{2}\tan\alpha \; . \tag{5}$$

The result of this replacement is a systematic uncertainty on the position of the entry point $x_0$:

$$\Delta x = x_0' - x_0 = \frac{D-L}{2}\tan\alpha \; . \tag{6}$$

The track depth $d$ is determined by the relation

$$d = \frac{x_i - x_0}{\tan\alpha} \; . \tag{7}$$

The track depth $d$ is measured in the centre $x_i$ of each pixel ($i = 1,2,3,...$). The depth of the track $d$ is calculated for every pixel and filled into a histogram. To determine the depletion depth the following error function is fitted to the falling edge of the distribution:

$$f(D_f - x) = 1 - \left( \frac{a}{\sqrt{2\pi}\cdot b} \int_0^{D_f - x} \exp(-t^2)dt \right) \; . \tag{8}$$

a,b and $D_f$ are parameters determined by the fit. $D_f$ is the inflection point of the function and is defined as the depletion depth. An example of the fit is shown in Figure 8. To estimate the depletion depth D, two major corrections have to be applied.

**Correction for threshold and angle dependence** The measured depletion depth depends on the discriminator threshold and on the incidence angle of the corresponding track. For the correct estimation of the depletion depth, it is necessary to regard these effects. The maximum of the track depth $d$ is measured when the last pixel in the cluster is just above threshold. The inflection point is shifted systematically

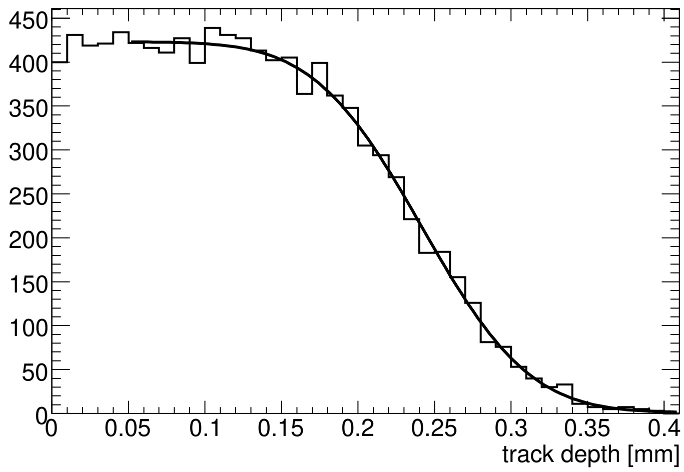


Figure 8: Track depth distribution for cosmics data taken without magnetic field.

to larger quantities, if the measured value of the maximum track depth is bigger than the real depleted depth. Therefore the correction for the fit value $D_f$ at a given incidence angle $\alpha$ is:

$$D' = D_f - \frac{\frac{P}{2} - X \cdot \sin(\alpha)}{\tan(\alpha)} \,. \tag{9}$$

P is the size of a pixel. The value X is the distance a particle has to travel in silicon until a pixel has collected enough charge carriers to reach the threshold. The size of a pixel in short pixel direction is 50 $\mu$m. The threshold is set to a value of 3950 electrons [**?**]. Hence the distance X is calculated to be 57 $\mu$m [**?**]. To ensure a fixed incidence angle it is necessary to divide the incoming particle tracks into different slices depending on the corresponding angle. Tracks with different angles are filled into different track depth histograms. One slice has a width of 0.2 radians. Function 8 is fitted to each histogram. An example of the outcome is shown in Figure 9. The estimated fit values $D_f$ are plotted versus the incidence angle. In this case the centre of the angle slices are used as the values of the incidence angles.

**Correction for the systematic uncertainty $\Delta x$** As soon as the depletion depth starts to decrease one has to take the systematic error $\Delta x$ into account (equation (6)). The local z position of the extrapolated cluster is located in the middle of the depleted depth. Since the depleted depth is unknown, the local z position is set to $\frac{L}{2}$. The systematic displacement of the entry point $x_0$ leads to a miscalculation of the depleted depth. Thus it is necessary to correct the estimated depletion depth a second time. The difference $Y$ between the measured value $D'$ and the corrected depleted depth $D$ is:

$$Y = \frac{L}{2} - \frac{D}{2} \,. \tag{10}$$

The outcome is the following correction for the measured value of the depleted depth:

$$D = 2 \cdot D' - L \,. \tag{11}$$

The sensor thickness $L$ is set to 250 $\mu$m.

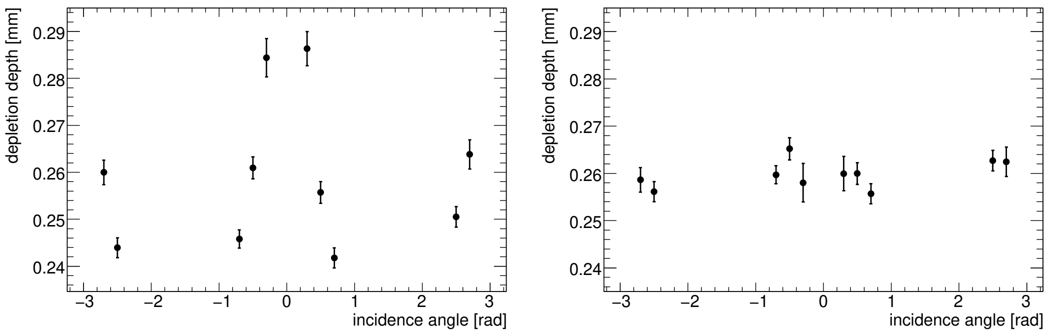


(a) $D_F$ (b) $D'$

Figure 9: Estimated fit values $D_F$ before (a) and $D'$ after (b) applying the correction.

#### 4.2.2 Track selection

In addition to the common cuts described in section **??** tracks with angles between 0.2 and 0.8 radians, or between 2.4 and 3.0 radians are used, as this is the range for which the measurement is sensitive to depletion depth. Also, only barrel hits for data without magnetic field are considered.

#### 4.2.3 Systematic uncertainties

Several systematical uncertainties have an influence on the extrapolated cluster position of the particle track, in addition to the known and corrected uncertainty $\Delta x$. The precision of the alignment has to be regarded. The detector has a resolution of 37 $\mu$m, after alignment [5]. Not every sensor has the same thickness. Also the thickness of the sensor on each module varies. The variation of the thickness has a mean value of 3 $\mu$m [6]. Furthermore, the bump bonds and the FE-Chips have a varying width. Because of these effects it is not possible to estimate the exact local position of the track in the pixel cluster. The result is a systematic uncertainty on the depletion depth of $\pm Z.Z$ $\mu$m.

Split clusters also affect the measurement. It is likely that not every pixel collects enough charge to reach the threshold, if the incoming track has a big incidence angle. Thus it is possible that the cluster is split. The size of these clusters is smaller than usually expected. As a result the depletion depth is underestimated. That is why the in section 4.2.2 described angle cut has to be applied.

#### 4.2.4 Results

**Monte Carlo Data** Simulated cosmics data is used for the following analysis. Figure 10 shows the results of the fits. Correction (9) has already been applied.

The weighted mean value is calculated to $\overline{D'} = (252 \pm 2 \pm Z)$ $\mu$m. The statistical error is determined by the fit. In order to determine the depletion depth, correction 11 is needed. The result of the measurement is a depletion depth of $\overline{D} = (254 \pm 4 \pm Z.Z)$ $\mu$m.

**Cosmics Data** Figure 11 shows the fit results of the analysis. Reprocessed cosmics are used for this analysis.

The result of the fits averages to $\overline{D'} = (259.7 \pm 0.8 \pm Z.Z)$ $\mu$m. Hence, the estimated depletion depth is $\overline{D} = (269 \pm 2 \pm Z.Z)$ $\mu$m.

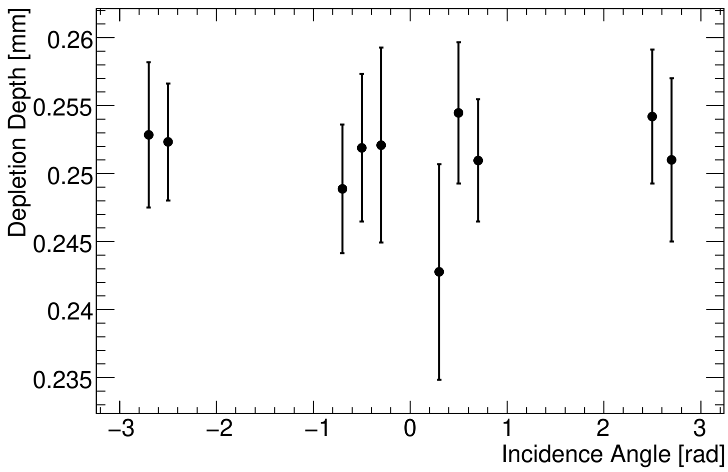


Figure 10: Estimated value $D'$ for simulated cosmics data.

#### 4.2.5 Discussion

*Prelinimnary:* Given that the sensors are not irradiated, one would expect a fully depleted detector. Thus the results should be in agreement with the thickness of the sensors. The sensor thickness in Monte Carlo cosmics data is set to 250 $\mu$m. Therefore the estimated depletion depth of the simulated data is consistent with the sensor thickness.

Referring to [6], the average sensor thickness is $(256 \pm 3)$ $\mu$m. The measured depth is 5% bigger than the mean value of the sensor thickness. However, the measured depletion depth is still in agreement with the measured sensor thickness, if the systematic error of Z.Z $\mu$m is taken into account. *more discussion...*

## 5 Conclusions

## 6 Acknowledgements

## References


[1] C. Jacoboni et al., Solid State Electronics **20** (1977) 77.

[2] I. Gorelov et al., Nucl. Instr. and Meth. A **481** (2002) 204.

[3] T. Lari, "Study of silicon pixel sensors for the ATLAS detector", PhD. Thesis, U. of Milano, CERN-THESIS-2001-028.

[4] T. Lari, "Lorentz angle variation with electric field for ATLAS silicon detectors", ATLAS note ATL-INDET-2001-004..

[5] Gray HM, Alignment of the ATLAS Inner Detector Tracking System, ATL-INDET-PROC-2008-005.

[6] The ATLAS Pixel Collaboration, ATLAS Pixel Detector Electronics and Sensors, 2008, JINST 3 P07007.

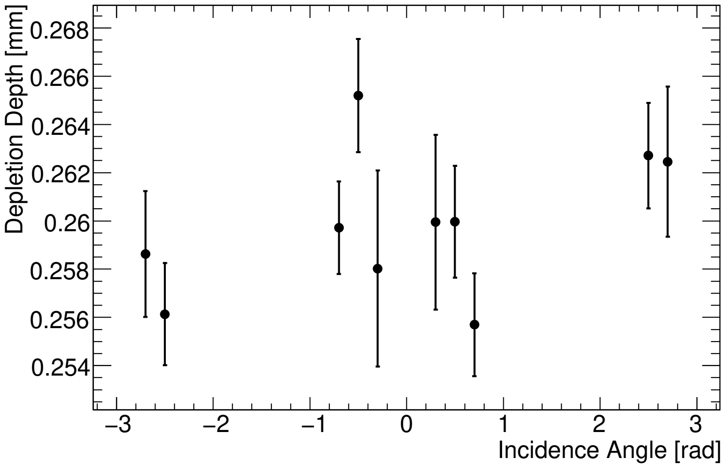


Figure 11: Estimated value $D'$ for cosmics data.